
Data report: trace element geochemistry of oceanic crust formed at superfast-spreading ridge, Hole 1256D¹

Yongjun Gao,² Jian Huang,² and John F. Casey²

Chapter contents

Abstract	1
Introduction	1
Methods and materials	1
Results	2
Acknowledgments	3
References	3
Figures	4
Tables	8

Abstract

This data report presents the bulk rock trace element compositions analyzed by inductively coupled plasma–mass spectrometry of the crustal rocks recovered during Integrated Ocean Drilling Program Expedition 309/312. The analyzed samples represent a subset of shipboard samples and a subset of samples collected and shared by a group of shipboard scientists.

Introduction

Integrated Ocean Drilling Program (IODP) Expedition 309/312 Hole 1256D, located in 15 Ma crust that formed at the East Pacific Rise during a period of superfast spreading (>200 mm/y), penetrated 1005 m into oceanic subbasement from the volcanic section to the upper portion of the plutonic complex (see the “[Expedition 309/312 summary](#)” chapter; Wilson et al., 2006). This data report presents the bulk rock trace element compositions of the basaltic rocks and gabbros recovered during the expedition. The analyzed samples represent a subset of shipboard samples that were analyzed onboard with inductively coupled plasma–atomic emission spectroscopy (ICP–AES) (shipboard AES samples) and a subset of samples collected and shared by a group of shipboard scientists (POOL samples). Shipboard AES samples were selected because they are the freshest and/or representative of rocks of each igneous unit. POOL samples were selected because they are representative of the various types of alterations and a few fresh alteration pairs (i.e., the fresh or less altered part and more altered part showing as alteration halos from the same sample).

Methods and materials

Onboard the *JOIDES Resolution*, selected representative whole-rock samples (shipboard AES samples) were cleaned by grinding off the outer surfaces with a diamond-impregnated disk to remove surface contamination by saw marks and altered rinds resulting from drilling. After sequential ultrasonication in trace-metal grade methanol, deionized water, and nanopure water, rocks were dried for 10–12 h at 110°C. The dry, clean samples were fragmented to small chips by crushing them between disks of Delrin plastic in a hydraulic press. The rock chips were then ground to a fine powder in a tungsten carbide mill.

¹Gao, Y., Huang, J., and Casey, J.F., 2009. Data report: trace element geochemistry of oceanic crust formed at superfast-spreading ridge, Hole 1256D. In Teagle, D.A.H., Alt, J.C., Umino, S., Miyashita, S., Banerjee, N.R., Wilson, D.S., and the Expedition 309/312 Scientists, *Proc. IODP*, 309/312: Washington, DC (Integrated Ocean Drilling Program Management International, Inc.). doi:10.2204/iodp.proc.309312.202.2009

²Department of Earth and Atmospheric Sciences, University of Houston, Houston TX 77204-5007, USA. Correspondence author: yongjungao@uh.edu



Expedition 309/312 POOL samples were prepared at the National Oceanography Centre, University of Southampton (United Kingdom). Following a comprehensive cleaning procedure, samples were crushed and powdered in a chrome-steel mill.

All samples were digested and analyzed in a clean laboratory. All reagents used were distilled and 18.2 M Ω ultrapure water was used. All gabbroic samples and those samples not completely digested on a hot plate were digested in high-pressure bombs. Accurately weighed samples (100 mg) were loaded into polytetrafluoroethylene (PTFE) cups and 1 mL 15.8N HNO₃ and 2 mL 24N HF were added. Samples were dried on a hot plate at 150°C to evaporate the SiF₄. Then 3 mL 12N HCl, 1 mL 16N HNO₃, and 4 mL 24N HF were added to the cups, which were then capped and placed in steel jackets and left in an oven at 180°C for 24 h. Samples were transferred to Savillex PTFE PFA beakers and dried to incipient dryness. After adding 4 mL 6N HCl, the Savillex beakers were placed on a hot plate at 100–120°C and dried to incipient dryness. Concentrated HNO₃ (2 mL) was added and the solution dried; this step was repeated two more times. After adding 4 mL of 8N HNO₃ to the beakers, the beakers were capped and left on a hot plate at 100°C until the samples were completely redissolved. Sample powders of basalt and dike rock were digested on a hot plate at 150°C using mixed HF and HNO₃ in Savillex PTFE PFA beakers and then dried on the hot plate at the same temperature. When the solution was completely dried, 2 mL 6N HCl was added to the beakers and the beakers were placed on hot plate to dry completely. After adding 4 mL 8N HNO₃, the beakers were capped and placed on a hot plate at ~100°C for 5–12 h. After transferring the sample solutions into acid cleaned polypropylene bottles, a known weight of internal standard solution was added and then diluted with water to a dilution factor of ~1000. The resulting solutions contained 2% HNO₃ and had a nominal internal standard concentration of 10 ppb. The internal standards used were Rh, In, Tm, Re, and Bi and enriched isotopes ⁶Li, ⁶¹Ni, ⁸⁴Sr, and ¹⁴⁵Nd, the mass of which covers the entire mass spectrum of the 35 analytes. This multiple internal standards technique provides the ability to monitor and correct the complex mass-dependent fractionations encountered in inductively coupled plasma–mass spectrometry (ICP-MS) multi-element analysis (Eggins et al., 1997). The samples were analyzed with a Varian ICP-MS at University of Houston (USA).

Data reduction was performed offline. During the course of an analytical run and with the introduction of different sample matrixes, it is very common

that the instrument sensitivity (defined as the number of counts per second obtained for a given concentration unit, e.g., cps/ppm) will drift. Accurate and precise data can only be obtained if the drift can be monitored and corrected. Raw intensities are corrected for drift, including mass-dependent drift, using combined external and internal standards. The United States Geological Survey (USGS) standard BHVO-2 was applied as an unknown sample to monitor the analytical precision and accuracy for each run. The elements Li, Be, Sc, Ti, V, Cr, Co, Ni, Cu, Zn, Ga, Rb, Sr, Y, Zr, Nb, Ba, La, Ce, Pr, Nd, Sm, Eu, Gd, Tb, Dy, Ho, Er, Yb, Lu, Hf, Ta, Pb, Th, and U were analyzed. Oxide interferences for rare earth elements (REEs), Hf, and Ta were corrected by applying a correction factor determined by the analysis of a 5 ppb pure Nd solution prior to each analytical run. Details of this technique is described by Hollocher (2008). Analytical precision represented by relative standard deviation is typically better than 5% (1.3%–4.6%), except for Pb which is 8.7% (Table T1). Analytical accuracy represented by the difference between analyzed and referenced concentrations in percentage is generally better than 5%, obtained by 57 replicate analyses (Table T1). Contamination introduced from crushing and powdering may cause significant bias of the accuracy. Therefore, the precision and accuracy evaluated from the repeated analysis of USGS standard BHVO-2 (Table T1) only refer to the dissolution and ICP-MS procedures.

Results

Results are presented in Tables T2 and T3.

There is no apparent difference in REE patterns and spider diagram patterns between analyzed shipboard AES samples and POOL samples (Figs. F1, F2), although the shipboard AES samples represent the freshest rocks in each igneous unit. This indicates that the original igneous property of typical immobile elements is well preserved. Positive Ta anomalies were observed only in shipboard AES samples and were most likely due to contamination from tungsten carbide during powdering. It has been shown that significant contaminants can be introduced from the grinding head during powdering (Webber et al., 2005). Tungsten carbide contains as much as 30 ppm Ta, which is 2 orders of magnitude higher than that in the analyzed samples. In contrast, Ta is not found in chrome steel, which explains the lack of Ta contamination in POOL samples. As no one sample was powdered by both methods, it is not possible to derive a direct evaluation of the contaminants from powdering at this stage. However, the

observation on Ta does show the importance of contamination from the grinding head.

Compared with normal mid-ocean-ridge basalt (NMORB), the basaltic rocks from Hole 1256D have more-developed negative Sr anomalies. The positive Sr anomaly first occurred near the sheeted dike–gabbro transition and becomes dominant in the plutonic section (Fig. F3). Compared with the basaltic rocks in the upper crust section and NMORBs, gabbros show depleted patterns (Figs. F1, F2).

Samples 312-19A and 312-19B (Sample 312-1256D-214R-1, Piece 9, 26–35 cm) represent a gabbro (312-19B)/oxide diorite (312-19A) contact. As shown in Figure F4, the oxide diorite has much more enriched trace element contents along with a strong negative Sr anomaly compared with the gabbro with which it is in contact. This may suggest that the oxide diorite was formed from the upward intrusion of the intercumulous liquids during the cooling of crystal mush that solidified to gabbros. The intrusion and crystallization of late stage melts derived from the intercumulous liquids have also been documented at slow-spreading ridges, such as Ocean Drilling Program Leg 118 Hole 735B (Dick et al., 2000; Natland and Dick, 2001).

Acknowledgments

This research used samples and/or data provided by the Ocean Drilling Program (ODP) and Integrated Ocean Drilling Program (IODP). ODP and IODP are funded by the U.S. National Science Foundation (NSF) and participating countries under management of Joint Oceanographic Institutions (JOI), Inc. These analyses were funded by a grant from the U.S. Science Support Program. Thanks go to Damon Teagle and his team for preparing and distributing the POOL samples. Thanks also go to the captain and crew of the *JOIDES Resolution* for their expertise, which made sample collection possible.

References

- Anders, E., and Grevesse, N., 1989. Abundances of the elements: meteoritic and solar. *Geochim. Cosmochim. Acta*, 53(1):197–214. doi:10.1016/0016-7037(89)90286-X
- Dick, H.J.B., Natland, J.H., Alt, J.C., Bach, W., Bideau, D., Gee, J.S., Haggas, S., Hertogen, J.G.H., Hirth, G., Holm, P.M., Ildefonse, B., Iturrino, G.J., John, B.E., Kelley, D.S.,

Kikawa, E., Kingdon, A., LeRoux, P.J., Maeda, J., Meyer, P.S., Miller, D.J., Naslund, H.R., Niu, Y.-L., Robinson, P.T., Snow, J., Stephen, R.A., Trimby, P.W., Worm, H.-U., and Yoshinobu, A., 2000. A long in situ section of the lower ocean crust: results of ODP Leg 176 drilling at the Southwest Indian Ridge. *Earth Planet. Sci. Lett.*, 179(1):31–51. doi:10.1016/S0012-821X(00)00102-3

Eggins, S.M., Woodhead, J.D., Kinsley, L.P.J., Mortimer, G.E., Sylvester, P., McCulloch, M.T., Hergt, J.M., and Handler, M.R., 1997. A simple method for the precise determination of ≥ 40 trace elements in geological samples by ICPMS using enriched isotope internal standardisation. *Chem. Geol.*, 134(4):311–326. doi:10.1016/S0009-2541(96)00100-3

Hollocher, K., 2008, http://minerva.union.edu/holloch/icp-ms/ree_corrections.htm.

Natland, J.H., and Dick, H.J.B., 2001. Formation of the lower ocean crust and the crystallization of gabbroic cumulates at a very slowly spreading ridge. *J. Volcanol. Geotherm. Res.*, 110(3–4):191–233. doi:10.1016/S0377-0273(01)00211-6

Sun, S.-S., and McDonough, W.F., 1989. Chemical and isotopic systematics of oceanic basalts: implications for mantle composition and processes. In Saunders, A.D., and Norry, M.J. (Eds.), *Magmatism in the Ocean Basins*. Geol. Soc. Spec. Publ., 42(1):313–345. doi:10.1144/GSL.SP.1989.042.01.19

Webber, E., Dyke, J.G., and Pappas, B., 2005. Grinding head contamination tests [poster presented at the Australian X-Ray Analytical Association Conference, Fremantle, Australia, 13–18 February 2005]. http://www.ga.gov.au/minerals/research/methodology/geochem/grind_contam_test.jsp

Wilson, D.S., Teagle, D.A.H., Alt, J.C., Banerjee, N.R., Umino, S., Miyashita, S., Acton, G.D., Anma, R., Barr, S.R., Belghoul, A., Carlut, J., Christie, D.M., Coggon, R.M., Cooper, K.M., Cordier, C., Crispini, L., Durand, S.R., Einaudi, F., Galli, L., Gao, Y., Geldmacher, J., Gilbert, L.A., Hayman, N.W., Herrero-Bervera, E., Hirano, N., Holter, S., Ingle, S., Jiang, S., Kalberkamp, U., Kerneklian, M., Koepke, J., Laverne, C., Vasquez, H.L.L., MacLennan, J., Morgan, S., Neo, N., Nichols, H.J., Park, S.-H., Reichow, M.K., Sakuyama, T., Sano, T., Sandwell, R., Scheibner, B., Smith-Duque, C.E., Swift, S.A., Tartarotti, P., Tikku, A.A., Tominaga, M., Veloso, E.A., Yamasaki, T., Yamazaki, S., and Ziegler, C., 2006. Drilling to gabbro in intact ocean crust. *Science*, 312(5776):1016–1020. doi:10.1126/science.1126090

Initial receipt: 28 August 2008

Acceptance: 28 May 2009

Publication: 30 October 2009

MS 309312-202

Figure F1. C1 chondrite-normalized (Anders and Grevesse, 1989) rare earth element patterns of crustal rocks, Hole 1256D. AES = atomic emission spectroscopy.

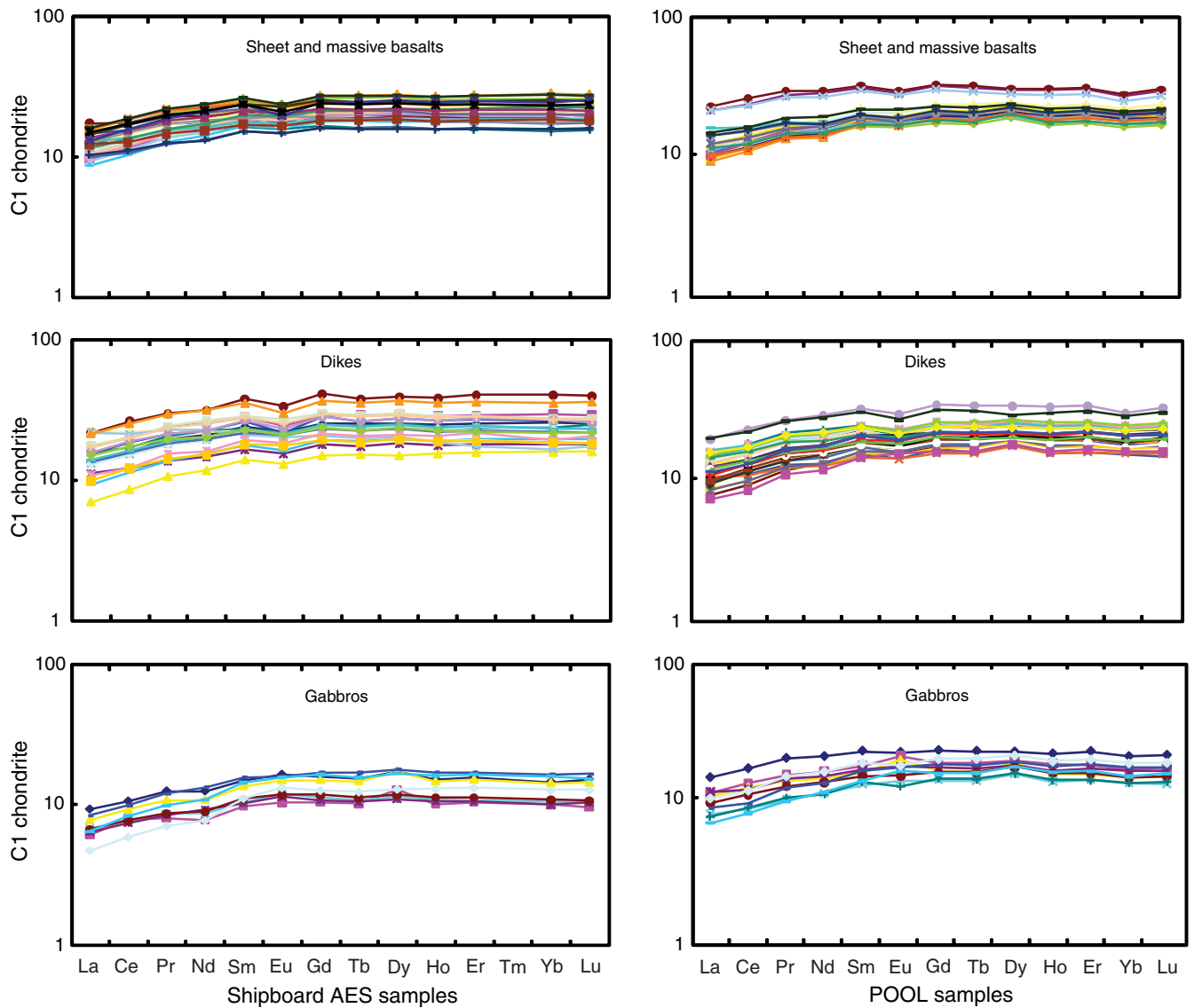


Figure F2. C1 chondrite-normalized multielement diagrams of crustal rocks, Hole 1256D. Red dashed line = normal mid-ocean-ridge basalt (Sun and McDonough, 1989). AES = atomic emission spectroscopy.

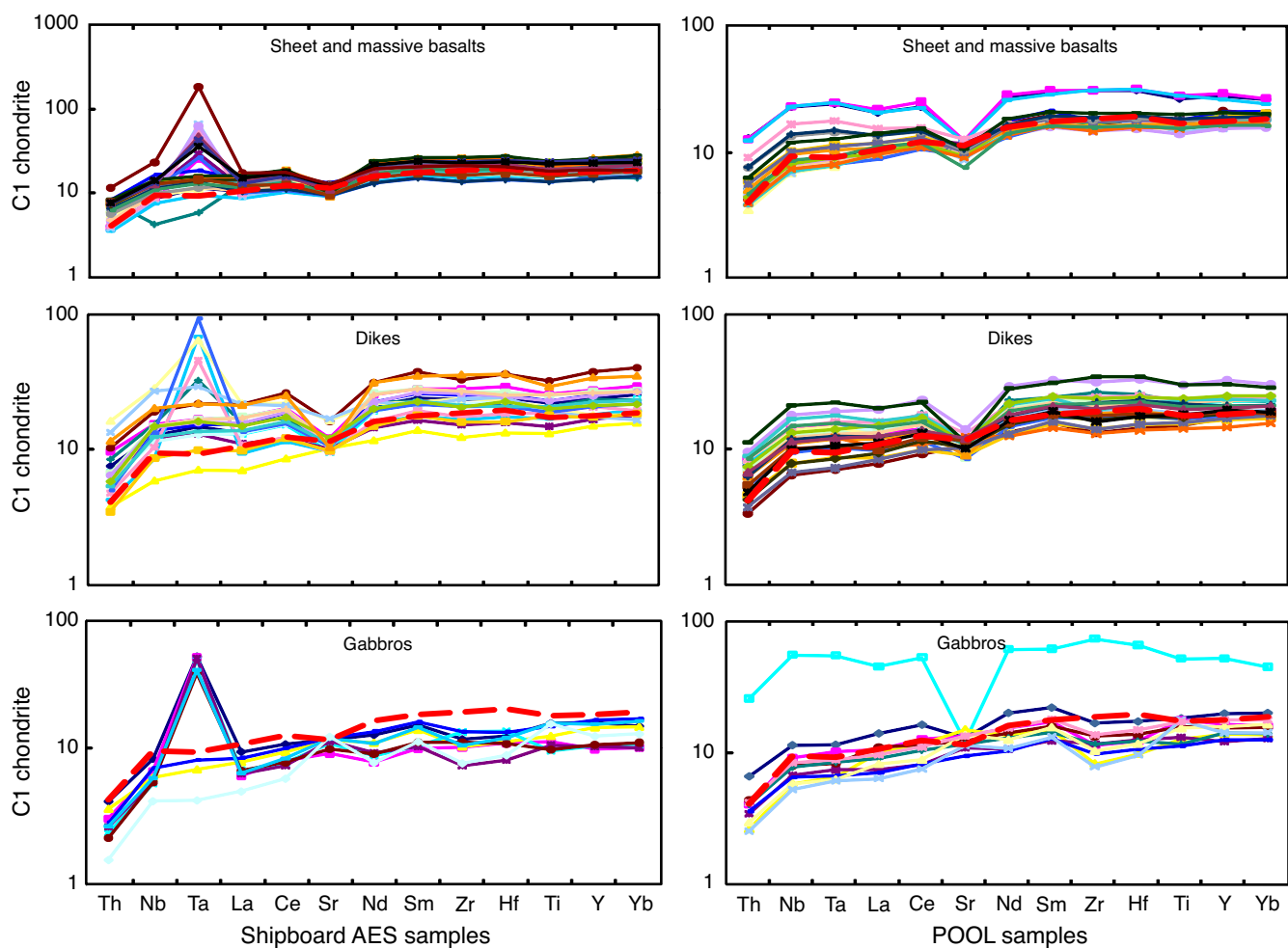


Figure F3. Downhole variation of bulk rock Sr anomalies of crustal rocks, Hole 1256D. $Sr^* = (Sr_N / \sqrt{Ce_N \cdot Nd_N}) - 1$, where N = C1 chondrite-normalized value.

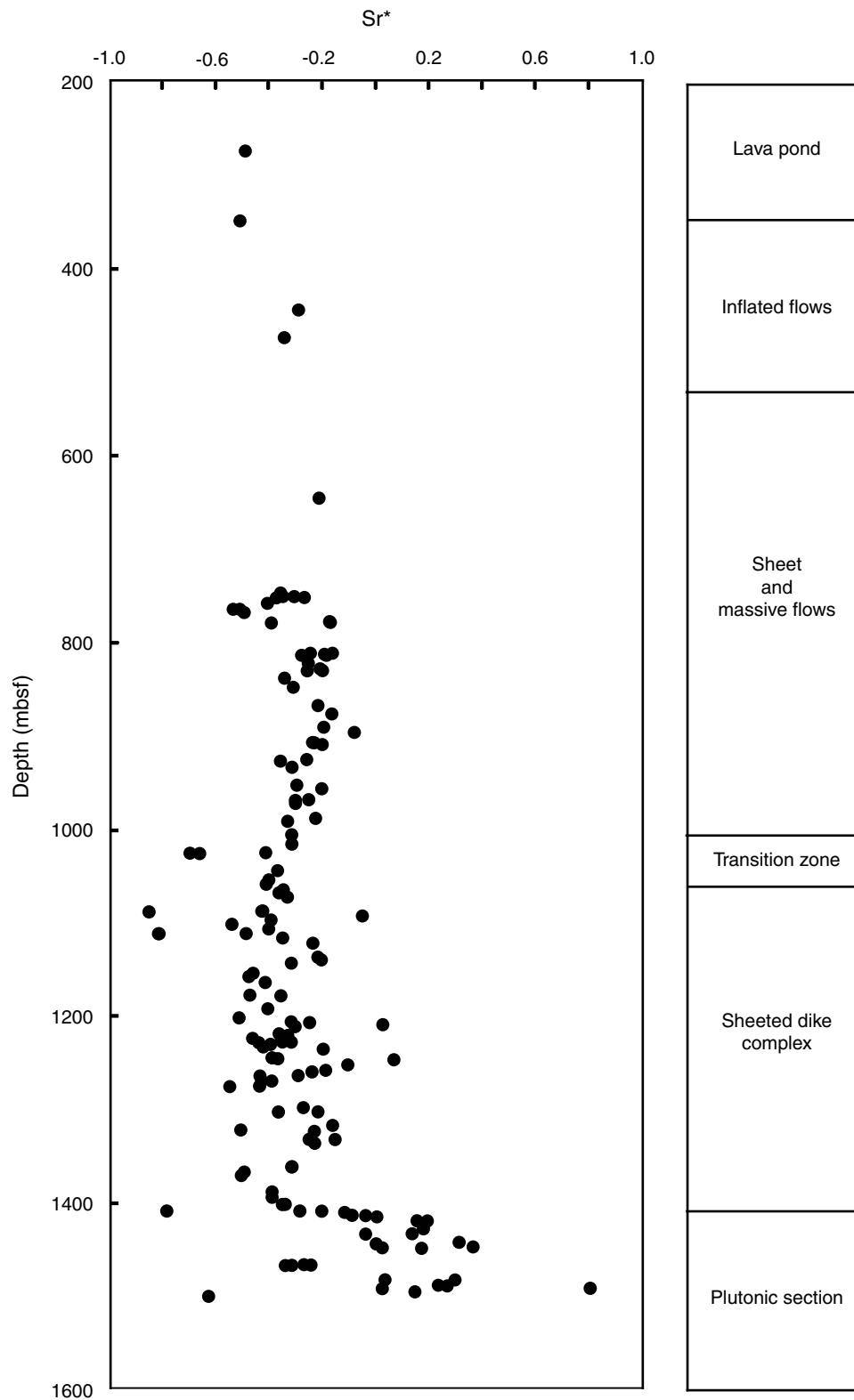


Figure F4. C1 chondrite-normalized multielement diagram of bulk rock (Sample 312-1256D-214R-1, Piece 9, 26–35 cm) representing an oxide diorite (Sample 312-19A)/gabbro (Sample 312-19B) contact.

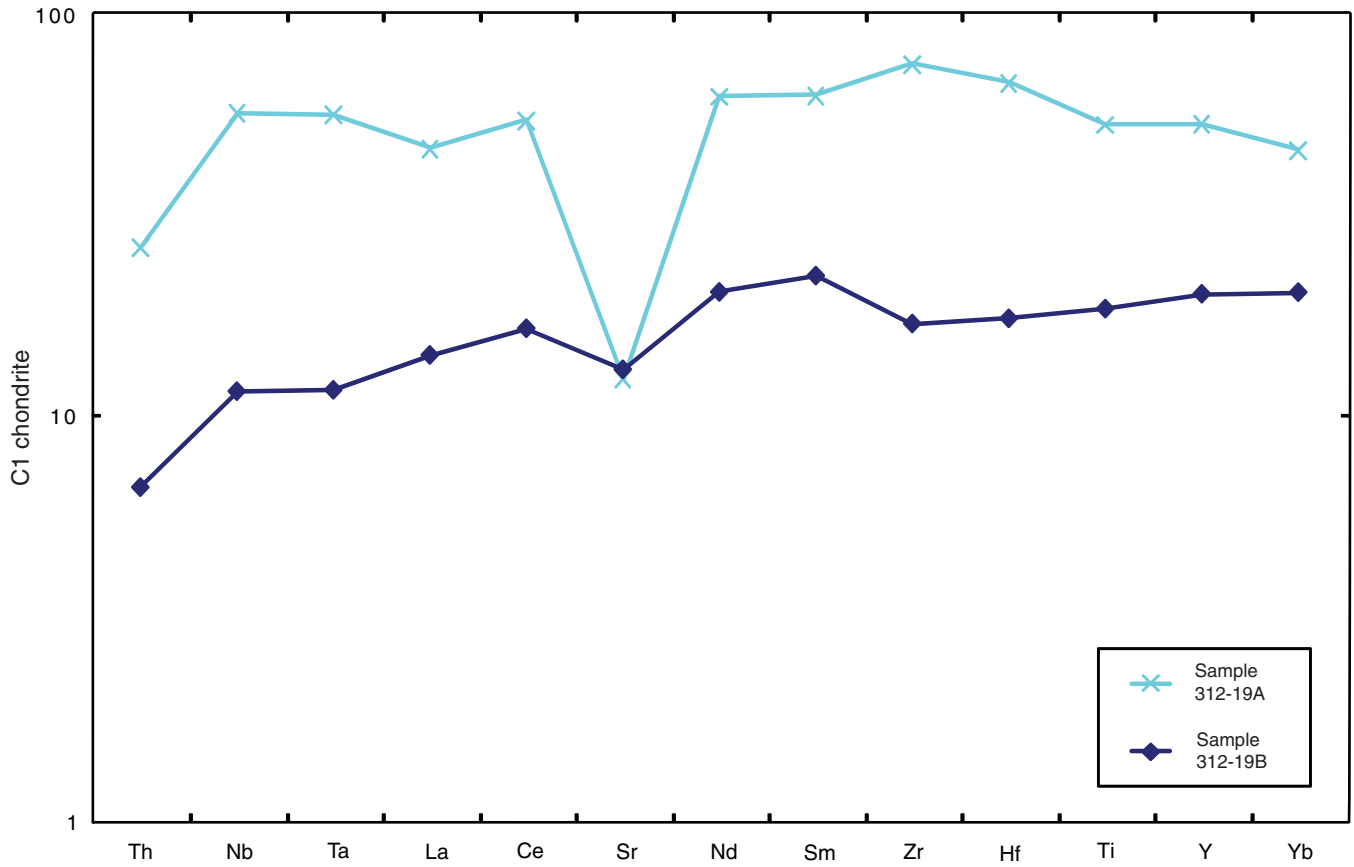


Table T1. Trace element concentrations, United States Geologic Survey standard BHVO-2. (See table notes.)

Element	REF (ppm)	Mean (ppm)	RSD (%)	Difference (%)
Li	4.33	4.30	2.0	-0.6
Be	1.03	1.00	4.6	-3.0
Sc	32.2	32.5	3.4	0.9
Ti	16,366	16,589	2.5	1.4
V	324	323	1.9	-0.2
Cr	310	311	1.7	0.3
Co	46.5	46.5	1.4	-0.1
Ni	120	120	1.5	0.0
Cu	124	124	1.6	0.5
Zn	106	105	1.8	-0.5
Ga	22.6	22.8	1.6	0.9
Rb	9.27	9.29	2.7	0.3
Sr	395	395	2.9	-0.1
Y	25.5	25.5	1.4	-0.3
Zr	172	172	1.5	0.0
Nb	18.0	18.0	2.2	0.1
Ba	133	135	1.6	1.3
La	15.2	15.4	1.7	1.3
Ce	37.4	37.7	1.3	0.8
Pr	5.35	5.40	1.3	0.8
Nd	24.4	24.5	1.7	0.3
Sm	6.10	6.14	1.3	0.6
Eu	2.04	2.05	1.3	0.2
Gd	6.16	6.19	2.1	0.5
Tb	0.91	0.92	1.7	0.2
Dy	5.29	5.35	1.9	1.3
Ho	0.98	0.98	1.4	-0.1
Er	2.47	2.49	1.6	0.9
Yb	2.02	2.02	1.9	0.1
Lu	0.28	0.28	1.3	0.1
Hf	4.34	4.34	1.5	-0.2
Ta	1.13	1.13	1.8	-0.3
Pb	1.54	1.56	8.7	1.4
Th	1.19	1.19	2.8	0.4
U	0.41	0.41	2.5	-0.5

Notes: REF = GeoReM preferred values taken from georem.mpch-mainz.gwdg.de/. For mean, $N = 57$. RSD = relative standard deviation.

Table T2. Trace-element compositions of crust rocks at Hole 1256D recovered during Leg 309 and Leg 312 (shipboard samples). This table is available in an [oversized format](#).

Table T3. Trace-element compositions of crust rocks at Hole 1256D recovered during Leg 309 and Leg 312 (POOL samples). This table is available in an **oversized format**.